Thermodynamic optimization of heat exchanger circuitry via genetic programming

Thermodynamic optimization of heat exchanger circuitry via genetic programming

Niccolo Giannetti[a], Adriano Milazzo[b], John Carlo S. Garcia[c], Cheol Hwan Kim[d], Yuichi Sei[e], Koji Enoki[f], Kiyoshi Saito[g]

[a] Waseda Institute for Advanced Study, Waseda University, Tokyo 169-8050, Japan

[b] Department of Industrial Engineering, University of Florence, Florence 50139, Italy

[c] Department of Mechanical Engineering, University of the Philippines, Quezon City, 1101, Philippines

[d] Research Institute for Science and Engineering, Waseda University, Shinjuku-ku, Tokyo, 169-8555, Japan

[e] Department of Informatics, The University of Electro-Communications, Tokyo 182-8585, Japan,

[f] Department of Mechanical and Intelligent Systems Engineering, The University of Electro-Communications, Tokyo 182-8585, Japan,

[g] Department of Applied Mechanics and Aerospace Engineering, Waseda University, Tokyo 169-8555, Japan,

*Corresponding author: niccolo@aoni.waseda.jp

Abstract

In this study, an evolutionary thermodynamic technique was developed for the optimization of heat exchanger circuitry. The developed technique is capable of handling the implementation of genetic operators with an unrestrained number and location of splitting and merging nodes while ensuring circuitry feasibility and manufacturability. The optimization tool was used to clarify the optimal heat transfer features in relation to the thermophysical and transport characteristics of the refrigerant and to provide a thermodynamic interpretation of the optimization results to extract general design guidelines. Circuitry optimization was conducted for a finned-tube evaporator with 36 tubes integrated into a thermodynamic cycle under a given cooling capacity, superheating degree, and boundary conditions representative of air-conditioning applications. The consistency between the minimum entropy generation and the maximum coefficient of performance (COP) was demonstrated under these settings. Furthermore, the thermodynamic interrelations between the minimum entropy generation and maximum COP are discussed, and optimal heat exchanger configurations that maximize the performance of each refrigerant by minimizing friction and heat transfer irreversibility are proposed. Consequently, the evaporator outlet pressure increases, thus lowering the compression ratio and maximizing the COP. The proposed optimization method maximizes the benefits of low-GWP alternative refrigerants and shows that low-GWP zeotropic mixtures exhibit the largest benefit from the developed circuitry optimization procedure and may achieve a performance comparable to that of R32 and higher than that of R410A by approaching a Lorenz cycle operation.

Keywords: Thermodynamic analysis, Circuitry optimization, Zeotropic refrigerant mixture, Genetic programming

1. Introduction

In an effort towards transitioning to more environmentally friendly fluids, stricter ozone depleting potential (ODP) and global warming potential (GWP) limitations have resulted in renewed interest in natural refrigerants and the development of new refrigerant blends such as zeotropic mixtures. Although natural refrigerants might be the most desirable long-term alternative, charge limitations and other selection criteria might restrict their use, and refrigerant blends might provide a broader spectrum of possible alternatives that are closer to optimal solutions. However, the performance assessment of such refrigerant blends and new low-GWP refrigerants remains inconclusive. For instance, zeotropic mixtures are refrigerants that introduce some thermodynamic benefits derived from low GWP values and characteristic temperature glide, yielding the possibility of realizing a Lorenz cycle operation. Nonetheless, in practice, these advantages remain unexploited because of two main challenges: (i) Challenging transport properties with a large pressure drop and limited transfer coefficient, which precludes taking advantage of the characteristic temperature glide. (ii) Ineffective design and optimization techniques that introduce unnecessary thermodynamic losses and increase the mean temperature difference between the primary and secondary fluids [1].

Accordingly, to maximize the advantages of next-generation refrigerants, heat exchangers have a critical influence on the overall system performance and represent the system's thermal interface in specific application cases. Therefore, heat exchangers are key components that must be optimized to maximize the heat transfer and minimize thermodynamic losses. When designing smaller or more efficient heat exchangers, the limited airside heat-transfer coefficient represents the main resistance, and previous studies have focused on developing high-performance airside transfer surfaces [2–5]. Complementarily, the heat exchanger performance is the result of a combination of airside heat transfer and two-phase refrigerant heat, mass, and momentum transfer. There is a large variability in the thermophysical properties of the refrigerant side, accompanied by large variations in the local heat-transfer coefficient, local pressure drop, and local temperature difference between the refrigerant and air. These complexities exhibit different characteristics and intensities with respect to the different refrigerant properties and structural characteristics of the heat exchanger, such as the splitting and merging junctions, which define the local refrigerant flow rate and quality distribution. Consequently, more efficient and compact heat exchangers may be obtained by acting on the refrigerant circuitry to optimize the local thermal matching between the air and refrigerant temperatures, pressure drop, and heat-transfer coefficient in relation to the refrigerant characteristics for given system requirements [6]. However, the effort presently required to design heat exchangers with high thermal effectiveness is significant for manufacturers, requiring trial-and-error procedures and multiple expensive experimental tests.

This study focuses on refrigerant circuitry optimization as an effective way to influence the local temperature difference, pressure drop, and heat-transfer coefficient. Accordingly, genetic programming and traversing algorithms from graph theory are integrated with a numerical simulator to establish an automatized refrigerant-circuitry optimization technique that can handle the implementation of genetic operators with unrestrained number and location of splitting and merging nodes, while ensuring circuitry feasibility and manufacturability. The developed optimization method and the thermodynamic analysis of the results provide insights into the optimal heat transfer features of the system, where entropy generation is used as a design tool for the advancement of next-generation refrigerants.

The remainder of this paper is organized as follows. Section 2 provides a brief overview of the adopted numerical model of the heat exchanger, the circuitry optimization algorithm, and the optimization settings. Results are presented in Section 3, which discusses their thermodynamic interpretation and application for refrigerant performance evaluation when optimal heat exchanger topologies are adopted to take advantage of the thermodynamic benefits of each refrigerant. Finally, Section 4 draws the main conclusions.

2. Simulator and optimization tool

Extensive research efforts have been dedicated to the optimization of refrigerant circuitry. For instance, Liang et al. [7] investigated the effect of circuitry branching on the heat transfer and pressure drop characteristics; however, their study was limited to refrigerant circuitry with two branches. Subsequent research adopted evolutionary search methods such as genetic algorithms to deal with the extensive search space of possible tube connections. Domanski [8–10] developed a public-domain simulation platform to analyze finned-tube evaporators and condensers with complex circuitry arrangements. This model was further developed by Lee et al. [11], who considered a two-dimensional airflow distribution. Liang et al. [12] evaluated the performance of different refrigerant circuits using an exergy destruction analysis. Ploskas et al. [13] applied derivative-free optimization algorithms to the simulation and design tools developed by Jiang et al. [14]. Li et al. [15] developed a new integer-permutation-based genetic algorithm (IPGA) for circuitry optimization with manufacturability and operating constraints. Recently, Ishaque and Kim [16] proposed an optimization algorithm based on knowledge- and permutation-based modules to maximize the heat-transfer capacity while providing feasible and efficient refrigerant circuits. However, no conclusive optimization tool has been established because of the following two main challenges:

- Unsuitable mathematical representations of the refrigerant circuitry, which provide non-bijective relations between the physical circuitry and its mathematical representation, and are unable to detect unfeasible circuitries;

- Limited search spaces, where only simple circuits with predetermined locations and numbers of splits are considered [17, 13, 18] owing to ineffective evolutionary techniques that are unable to manage genetic operators in complex circuitries.

Therefore, except for simplified analytical approaches that consider constant transport properties along the refrigerant flow [19-20], these efforts do not provide answers for defining the number and location of splitting and merging within refrigerant circuitry.

To overcome these issues, this study relies on the concept of graph theory to develop a suitable mathematical representation of refrigerant circuitry to construct a one-to-one relationship with physical circuitry and recognize unfeasible features. In addition, genetic programming was used to apply genetic operators to an unrestrained search space of complex circuitry with an arbitrary number and location of split/merge junctions. A simulator was developed around a bijective mathematical representation of the refrigerant circuitry, called the tube–tube adjacency matrix (described in [21]), and related constraints were formulated to ensure the coherence and feasibility of the circuitry during the evolutionary search. Consequently, a novel evolutionary algorithm for refrigerant circuit optimization was developed [22].

Circuitry formulation

The tube-tube adjacency matrix (Fig. 1) was developed in a previous study [21]. It consists of a square and anti-symmetric matrix that contains all information on refrigerant circuitry, which is employed in setting the governing equations for each tube, and is connected with traversing algorithms to detect unfeasible connections (for more details, please refer to [21]).

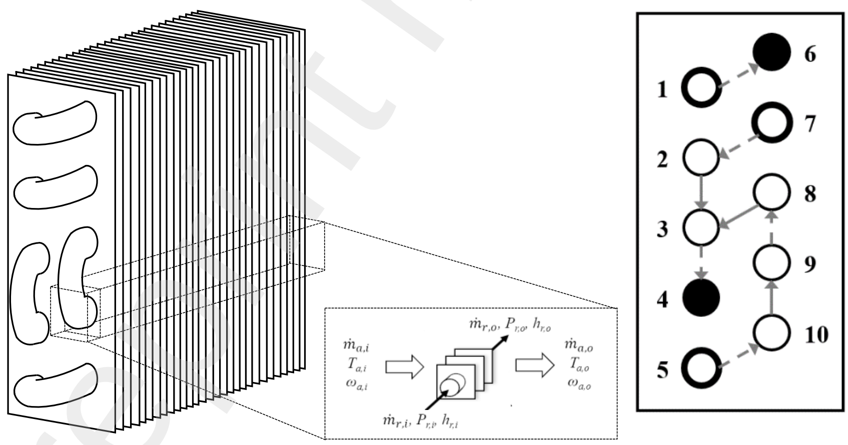

Reference	Connected tubes									
	1	**2**	**3**	**4**	**5**	**6**	**7**	**8**	**9**	**10**
1	0	0	0	0	0	1	0	0	0	0
2	0	0	1	0	0	0	-1	0	0	0
3	0	-1	0	1	0	0	0	-1	0	0
4	0	0	-1	0	0	0	0	0	0	0
5	0	0	0	0	0	0	0	0	0	1
6	-1	0	0	0	0	0	0	0	0	0
7	0	1	0	0	0	0	0	0	0	0
8	0	0	1	0	0	0	0	0	-1	0
9	0	0	0	0	0	0	0	1	0	-1
10	0	0	0	0	-1	0	0	0	1	0

Fig. 1 Schematic of a finned-tube heat exchanger and its corresponding tube-tube adjacency matrix

The direct application of genetic operators to the chromosomes of parent circuitries may result in unfeasible and nonphysical offsprings. As a result, the generation of nonphysical circuitries is excluded based on the formulation of the corresponding topology constraints, including non-connected tubes, unfeasible internal loops, and upstream flows of a merge coming from opposite sides of the heat exchanger (for details regarding the mathematical formulation of these limitations, please refer to [22] and [23]).

Furthermore, two manufacturability constraints in the circuitry arrangements were considered (Fig. 2): U-bends longer than the prescribed manufacturing limit and heat exchanger outlets on different sides of the heat exchanger. The limitation of possible gene combinations using these constraints can significantly reduce the size of the search space and facilitate the evolutionary algorithm convergence.

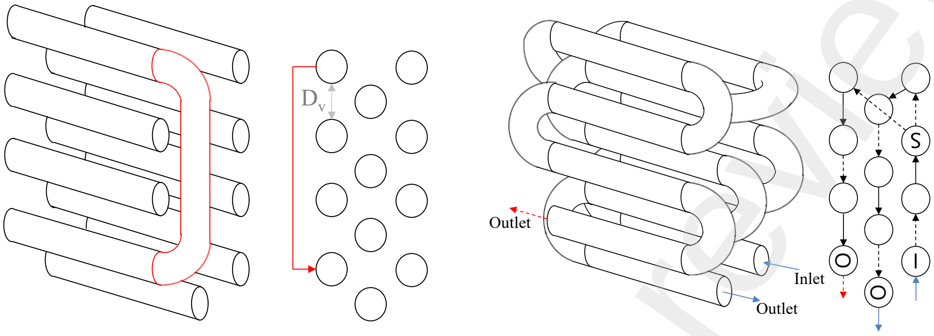

Fig. 2 Manufacturability constraints

Numerical model

The model was developed by considering both the physical accuracy required to capture complex two-phase heat transfer and pressure drop characteristics, as well as the calculation cost for effective integration with evolutionary algorithms. Accordingly, a tube-by-tube approach was considered along with the following assumptions: steady state, negligible change in potential and kinetic energy, negligible heat transfer in the tube bends, and uniform air distribution. The heat transfer and pressure drop of the air were modeled using the Kim-Youn-Webb [24,25] correlations for the airside heat-transfer coefficient and pressure drop. The refrigerant-side heat transfer was modelled using Shah correlations (1982) [26] and (2015) [27] for the saturated boiling heat transfer of pure refrigerants and zeotropic mixtures, respectively, and the Dittus-Boelter equation [28] was used for the single-phase heat-transfer coefficient. Müller–Steinhagen and Heck [29] adopted the two-phase refrigerant pressure gradient. Popiel and Wojtkowiak [30] is used to calculate the single-phase pressure drop in U-bends, while Domanski and Hermes [31] used a two-phase flow. The model was validated through dedicated experimental tests on a 28-tube evaporator using R410A. The simulated overall heat duty and pressure drop were within 7% and 8% of the experimental values, respectively. In addition, the accuracy of the local temperature distribution was confirmed [21,22].

Circuitry optimization algorithm

Evolutionary algorithms have been widely used to solve optimization problems owing to their robustness and flexibility in deriving solutions in complex spaces. The developed optimization algorithm is a path generation algorithm based on genetic programming, which applies genetic operators to tree structures used as genotypes, while overcoming limitations related to the management of unrestricted numbers and locations of splits and merges. In such tree structures, each node corresponds to a unique tube and is generated according to rules designed to exclude unfeasible circuits. Each tree (circuit) starts with root nodes (inlet tubes) and ends with leaves (outlet tubes). A tree can branch into subtrees if splits and merges exist within the circuit. The depth of the tree is equal to the number of nodes that must be traversed from the root node to reach the leaf. The proposed algorithm consists of five main phases: (I) initialization, (II) selection, (III) crossover, (IV) mutation, and (V) application of physical constraints (as illustrated in Fig. 3).

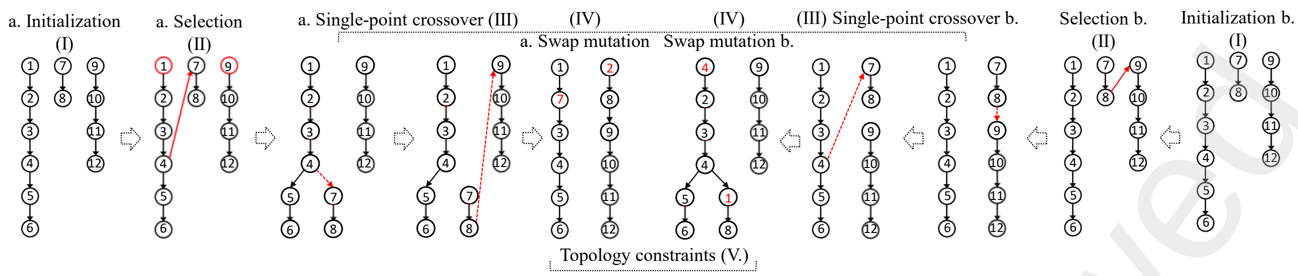

Fig. 3 Schematic representation of the optimization algorithm.

The search process is based on the first initialization of the population and its evolution towards the subsequent generations. The population individuals from each generation are evaluated on the basis of a fitness function (hereby referred to as "objective function") and the selection of parents is based on the roulette wheel method [32], where the probability of an individual to be chosen as a parent is proportional to its fitness value. Consequently, genetic operations such as crossover and mutation are applied to the parent circuits to obtain new offspring circuits. Finally, it is ensured that the resulting tree structures satisfy the physical and manufacturability constraints of the actual refrigerant circuits of the heat exchangers, and the generated structures are selected for the next generation. This process is repeated until convergence to the optimization criterion or until the maximum number of generations is reached.

Objective function and optimization settings

Irreversibility assessment for an efficient heat exchanger design has been recognized since the theoretical work of Bejan [33], complemented by Grazzini and Gori [34], and has been extensively applied to different technologies [35-36]. In this study, the local air and refrigerant states were calculated based on the numerical model presented above, while each tube's airside and refrigerant-side entropy generation were calculated using Eqs. (1) and (2), respectively. Here, $\dot{Q}_n$ represents the heat transfer rate at tube n. $\Delta P_{a,n}$, $\Delta P_{r,n}$, $\dot{m}_{a,n}$, and $\dot{m}_{r,n}$ are the airside pressure drop, refrigerant-side pressure drop, air flow rate, and refrigerant flow rate at tube n, respectively. $T_{r,n}$, $T_{w,n}$, and $T_{a,n}$ are the refrigerant-inlet, wall, and air-inlet temperatures, respectively.

$$S_{gen,a,n} = \dot{Q}_n \frac{T_{a,n} - T_{w,n}}{T_{a,n}T_{w,n}} + \dot{m}_{a,n}\frac{v_{a,n}}{T_{a,n}}\Delta P_{a,n} \tag{1}$$

$$S_{gen,r,n} = \dot{Q}_n \frac{T_{w,n} - T_{r,n}}{T_{w,n}T_{r,n}} + \dot{m}_{r,n}\frac{v_{r,n}}{T_{r,n}}\Delta P_{r,n} \tag{2}$$

Accordingly, the objective function adopted to evaluate the fitness of the circuits generated by the evolutionary path-generation algorithm is the minimum total entropy generation, defined as follows:

$$S_{gen} = \sum_{n=1}^{N} \left(\dot{Q}_n \frac{T_{w,n} - T_{r,n}}{T_{w,n}T_{r,n}} + \dot{Q}_n \frac{T_{a,n} - T_{w,n}}{T_{a,n}T_{w,n}} + \dot{m}_{r,n}\frac{v_{r,n}}{T_{r,n}}\Delta P_{r,n} + \dot{m}_{a,n}\frac{v_{a,n}}{T_{a,n}}\Delta P_{a,n} \right)_n \tag{3}$$

The proposed evolutionary algorithm was applied to optimize the evaporator within an air-conditioning cycle to evaluate the performance of different refrigerants. Three representative refrigerants for air-conditioning applications were investigated: a pure refrigerant (R32), a near-azeotropic mixture (R410A), and a low-GWP zeotropic mixture (R454C). The search for refrigerant circuitries approaching the optimal results for a given objective function was performed for a 36-tube evaporator with 12 tube rows and the transfer surface features previously adopted by Domanski et al. [17] (Table 1). The single-split circuit configuration shown in Fig. 4 [17] was used as the baseline circuit for comparison. In the schematic, the inlet tubes are represented by thick-bordered circles, outlet tubes by "O" symbols, and splits by "S" symbols. The solid lines represent the return bends on the front side of the heat exchanger, while the return bends on the back side are represented by dashed lines.

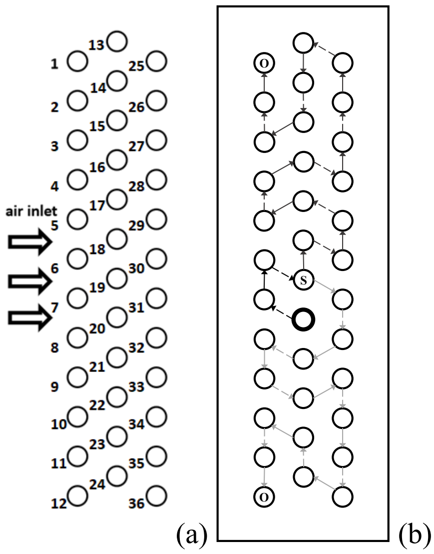

Fig. 4 (a) Evaporator configuration and (b) baseline circuitry from [14].

Table 1. Geometric features of the evaporator

Tube outer diameter	0.01 m
Tube inner diameter	0.0092 m
Tube length	0.5 m
Tube vertical pitch	0.0222 m
Tube transversal pitch	0.0254 m
Fin spacing	0.002 m
Fin thickness	0.0002 m

The input parameters, such as the return room air temperature, adiabatic efficiency of the compressor, air inlet conditions, and inlet enthalpy of the evaporator, defined isenthalpically by the condensing temperature and subcooling degree, are summarized in Table 2. For zeotropic refrigerant mixtures, the saturation pressure is determined with reference to the average temperature between the boiling and dew points. The iterated values are the local refrigerant state and flow rate at each tube, in addition to the total refrigerant and air flow rates, and the inlet pressure to the evaporator while converging to a given cooling capacity, supply air temperature, and superheating requirements.

Table 2. Operating conditions of the evaporator and condenser

Air inlet temperature (return air from the room)	26 °C
Air inlet pressure	101.325 kPa
Air outlet temperature (supply air to the room)	18 °C
Superheating degree	5 K
Cooling capacity	4,6,8,10 kW
Condensation temperature	45 °C
Subcooling degree	5 K
Compressor isentropic efficiency	0.85
Electric motor efficiency	0.85

For a given cooling capacity, the cycle coefficient of performance (COP) may be maximized by minimizing the compressor work. Under the calculation conditions listed in Table 2, the maximum cycle efficiency may be approached by searching for circuits that can maximize the evaporator outlet pressure (Eq. 4). This is consistent with the interpretation given by [20]

$$COP = \frac{\dot{Q}_e}{\dot{W}} = \frac{\dot{Q}_e}{\dot{m}_r \Delta h_{comp}} = \frac{\dot{Q}_e}{\dot{Q}_e / \Delta h_e \; \Delta h_{is} / \eta_{comp}} = \frac{1}{\frac{1}{\eta_{comp}} \frac{h(p_{cond}, s_{out,e}) - h(p_{out,e}, T_{sat}(p_{out,e}) + \Delta T_{sh})}{h(p_{out,e}, T_{sat}(p_{out,e}) + \Delta T_{sh}) - h_{in,e}}} \quad (4)$$

The evaporator outlet pressure may be maximized by reducing the pressure drop and mean temperature difference between the refrigerant and air, which can be achieved by minimizing the corresponding irreversible thermodynamic losses, namely, entropy generation arising from friction and entropy generation related to finite-temperature-difference heat transfer.

3. Results and discussion

The optimization runs adopted a population size of 500 times 100 generations; therefore, 50,000 circuitries were investigated for each run, according to the algorithm settings listed in Table 3. Finally, after reaching the maximum number of generations, the selected circuitry was further optimized using a tube-permutation procedure, which was directed to improve the thermal matching between the air and refrigerant temperature distribution. The corresponding optimization results are discussed to investigate the ability of the proposed optimization method to define suitable features of the refrigerant circuitry for different refrigerants and given operational requirements.

Table 3. Optimization search settings

Population size	500
Number of generations	100
Crossover probability	0.80
Mutation probability	0.005
Elitism probability	0.0005

Although Lee et al. [19] concluded that entropy generation minimization is an unsuitable method for optimal refrigerant circuit analysis because of the often-dominant effect of heat transfer on friction irreversibility, our results demonstrate consistency between minimum entropy generation and maximum COP when the calculation settings require convergence to a given output capacity requirement. The thermodynamic interrelations between minimum entropy generation and maximum COP were investigated and discussed, hence expanding the results of [20] to complex circuitries with unrestrained number and location of splitting junctions. Figure 5 illustrates the evolutionary progression of the search algorithm under the conditions described above for the optimization run conducted with R32 under a cooling capacity requirement of 6 kW. It can be seen that the optimization run progresses towards lower total irreversibility and more efficient heat exchanger configurations over 100 generations. More specifically, the results shown in Fig. 5 demonstrate that under the calculation conditions defined in Table 2, when the heat transfer irreversibility can be lowered at the expense of a moderately larger pressure drop and corresponding friction irreversibility, the total entropy generation at the corresponding evaporator can be minimized, and the cycle COP is maximized.

An optimization run was performed for each refrigerant and required cooling capacity. A near-optimum circuitry was obtained after each run. Figure 6 shows the circuitries obtained for the R32 calculations conducted in a range of 4–10 kW cooling capacity conditions. An interpretation of the schematics refers to the representation features in Fig. 4. Each heat exchanger configuration schematic is associated with a refrigerant flow path representation between the evaporator inlet and outlet. The latter provides a more immediate visualization of the number and location of split nodes as well as each branch length. It can be observed that the number of circuits and split locations vary according to the refrigerant and target capacity. Specifically, as the capacity increased for a given refrigerant, the split location moved upstream to limit the refrigerant pressure drop by reducing the local refrigerant flow rate. In addition, the latent heat of vaporization affects the flow rate required to achieve the target cooling capacity.

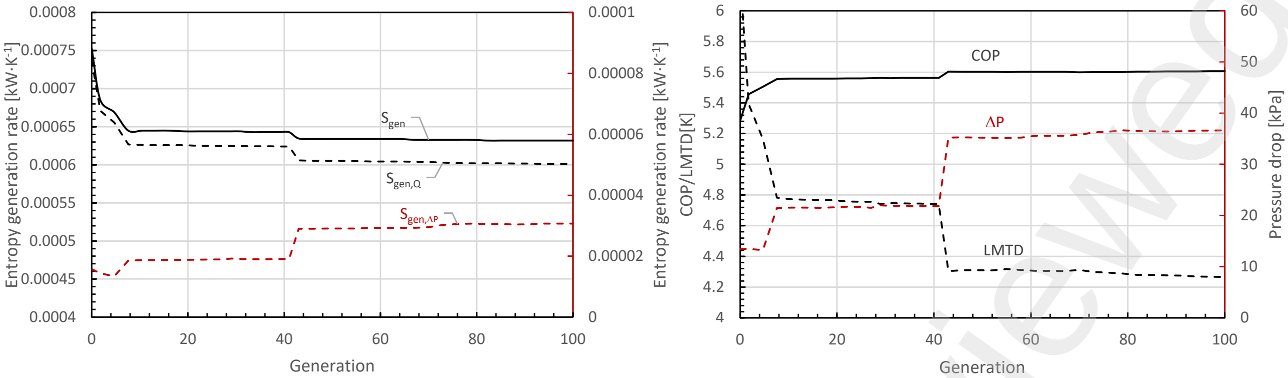

Fig. 5: Evolutionary entropy generation minimization and the corresponding COP, ΔP, and LMTD progression

Owing to its large latent heat among the three refrigerants, R32 required the lowest refrigerant flow rate to achieve its target capacity, whereas R454C required the highest flow rate. Accordingly, for a system employing R32, which also has the lowest viscosity among the refrigerants investigated in this study, the pressure drop can be controlled more easily with a lower number of parallel branches.

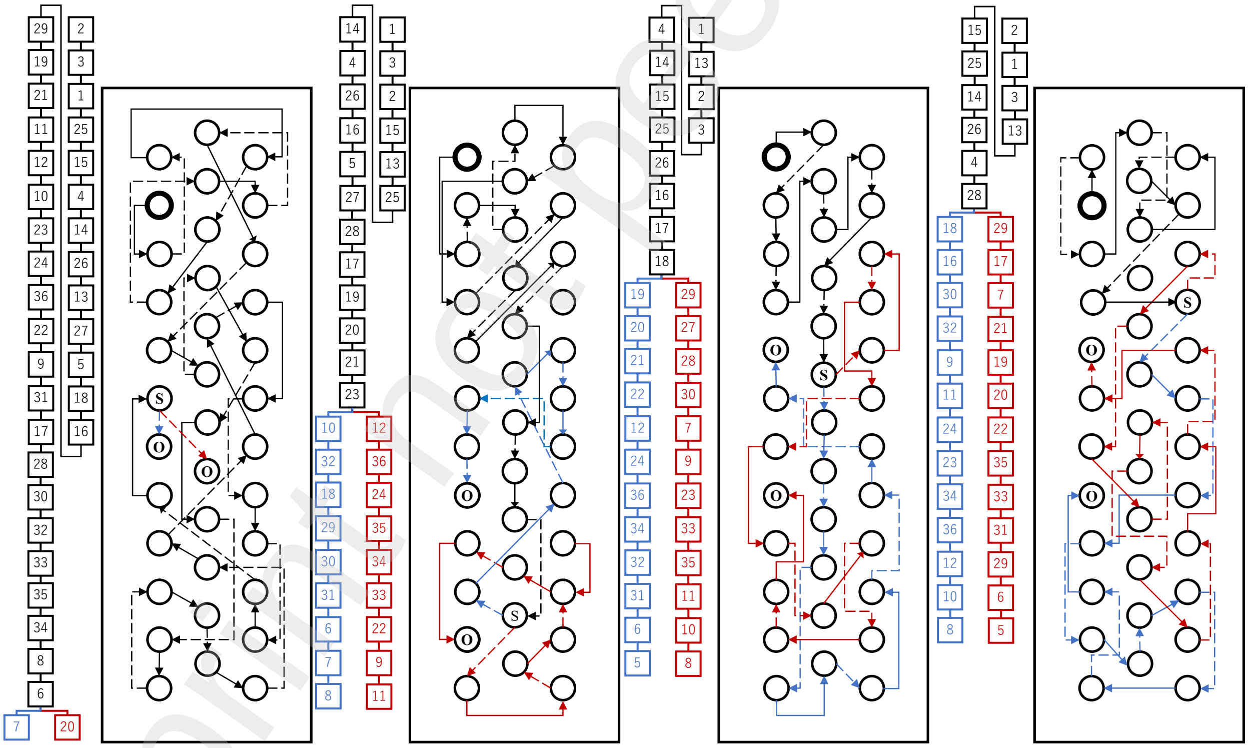

(a) (b) (c) (d)

Fig. 6: Optimized refrigerant circuitries for R32 under different cooling capacity conditions: (a) 4, (b) 6, (c) 8, and (d) 10 kW

Both the circuitry arrangement and splitting locations are consistent with the results discussed in [22], which adopted the corresponding simulation conditions while using the COP instead of total entropy generation as the objective function. This suggests that, under these optimization settings, the COP maximization in [22] was achieved by minimizing the total entropy generation at the evaporator. Additionally, the refrigerant circuitry determines the local temperature difference distribution between the air and refrigerant, which can be optimized to reduce the irreversible heat transfer losses according to the local refrigerant saturation temperature variations caused by the pressure drop or temperature glide or both of the zeotropic mixture. In this case, parallel flow characteristics are observed whenever the pressure drop reduces the local saturation temperature, while counterflow circuitry arrangements are associated with the superheated refrigerant flow parts of the optimized circuitries.

Figure 7 illustrates the local refrigerant pressure drop as well as the refrigerant and air temperatures along the refrigerant flow for R32 under a 10-kW cooling capacity simulation condition. The horizontal axis represents the refrigerant flow depth (number of tubes) between the evaporator inlet and outlet for each circuit branch. In addition, the air temperature distribution is arranged according to the refrigerant path to highlight the local temperature difference between the air and refrigerant; hence, it did not exhibit air flow continuity. In Fig. 7, the results for the representative one-split baseline serpentine presented in Section 2 (dashed lines) are compared with the optimized circuitries results (continuous lines). A notable feature of the optimized circuitries compared with the baseline is the presence of fewer tubes in the superheated refrigerant state. This improves the transfer surface utilization by minimizing the part of the transfer area that interfaces with the refrigerant flow with a low heat-transfer coefficient at the expense of a moderately high pressure drop and friction irreversibility. Consequently, the optimized circuit can achieve the same capacity while maintaining a smaller temperature difference between the refrigerant and air throughout the heat exchanger, which results in proportionally lower heat-transfer irreversibility and a more homogeneous heat-transfer rate distribution than the baseline circuitry, as shown in Fig. 8.

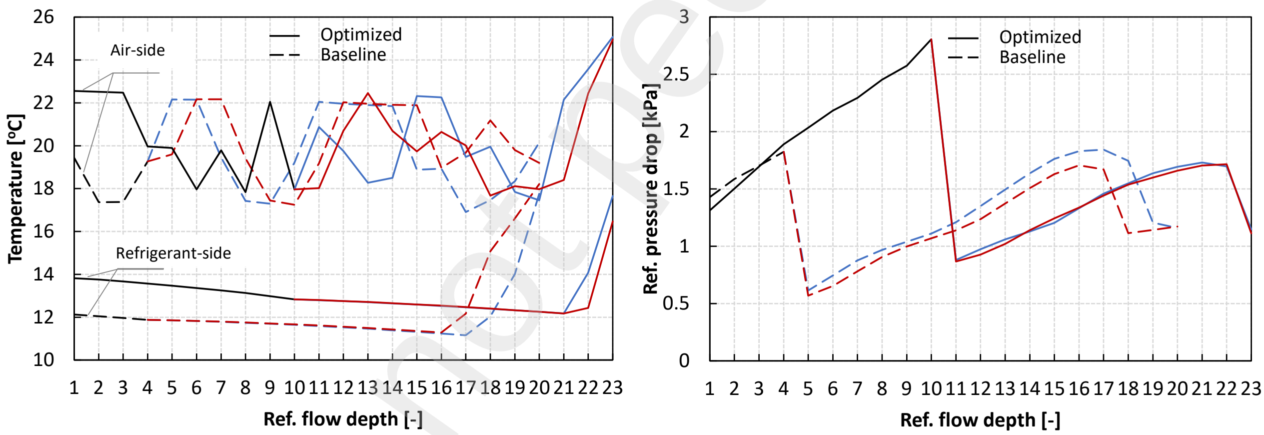

Fig. 7: Local refrigerant pressure drop and refrigerant/air temperatures for R32 for a 10-kW cooling capacity

The results obtained for the near-azeotropic mixture R410A for both optimized circuits were also analyzed (as shown in Fig. 9), as well as the effect on the local temperature and pressure drop distributions [22]. The optimized circuitries operate at a higher inlet evaporator pressure because the split location moves closer to the outlet, which results in a locally higher pressure drop and friction irreversibility, but also in a larger heat-transfer coefficient and smaller mean temperature difference between the refrigerant and air. Additionally, the rearrangement of the tube ordering improves the local temperature difference distribution between the air and refrigerant, which yields a lower finite-temperature-difference heat-transfer irreversibility. Because of the characteristic temperature glide and the different thermophysical and transport properties of zeotropic mixtures such as R454C, a different trend can be observed in the results obtained for such working fluids.

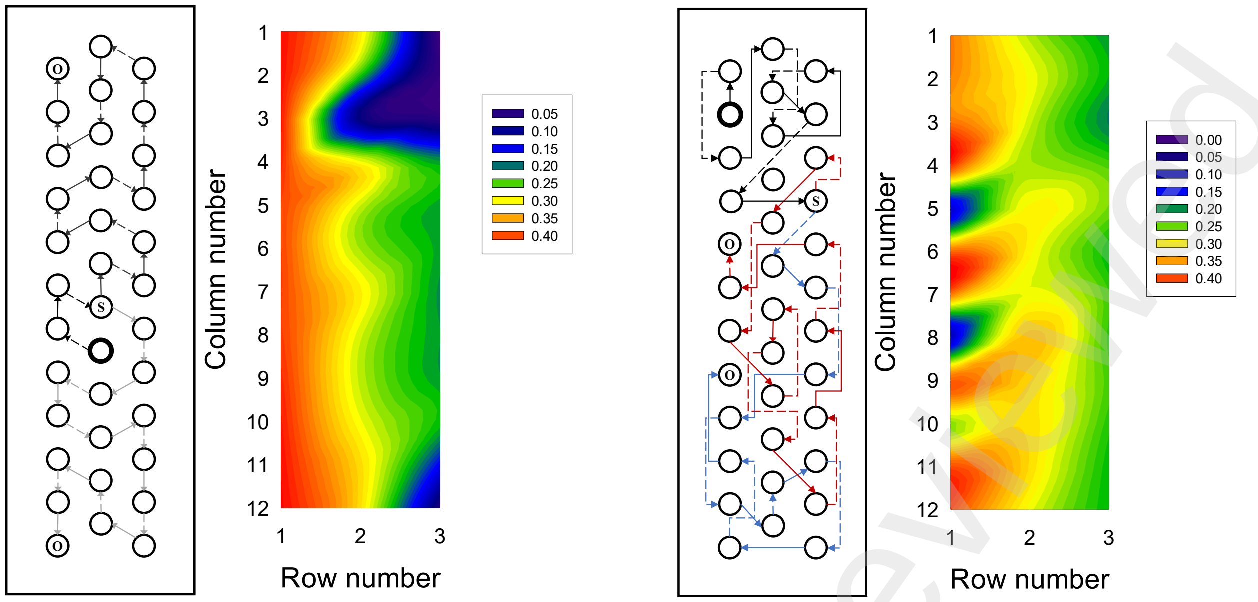

Fig. 8: Contours of the local heat transfer rate Q [kW] for the R32-refrigerant (a) baseline and (b) optimized circuitries for a 10-kW cooling capacity

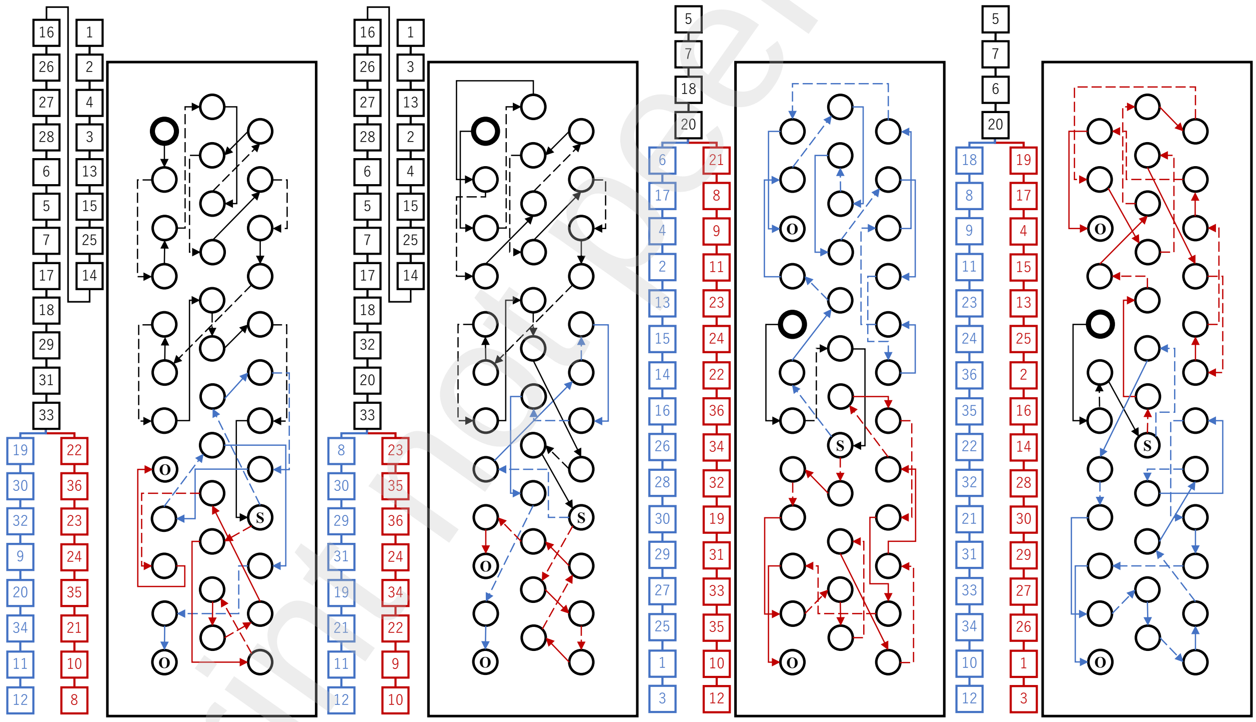

(a) (b) (c) (d)

Fig. 9: Optimized refrigerant circuitries for R410A under different cooling capacity conditions: (a) 4, (b) 6, (c) 8, and (d) 10 kW

Figure 10 shows the resulting optimized circuits for R454C, while Fig. 11 shows the local refrigerant temperature distribution and pressure drop of the baseline and optimized circuitries for simulations converging to 10-kW cooling capacity. Under these conditions, the optimized R454C circuitry features two parallel circuits and a lower pressure drop. Correspondingly, it operates at a marginally lower evaporator inlet pressure and a higher outlet pressure than the baseline circuitry. As shown in Fig. 11, the temperature glide could not be effectively utilized in the baseline circuitry because a large pressure drop reduces the characteristic temperature glide on the refrigerant side. In fact, the temperature of R454C in the baseline circuitry decreased before the split because of the pressure drop. Therefore, the optimized circuitry can take advantage of R454C's temperature glide by maintaining low pressure drop values and maximizing the effects of a counter-flow arrangement between the air and refrigerant flows. This configuration resulted in a more homogeneous local heat transfer rate $Q[i]$ distribution, as shown in Fig. 12.

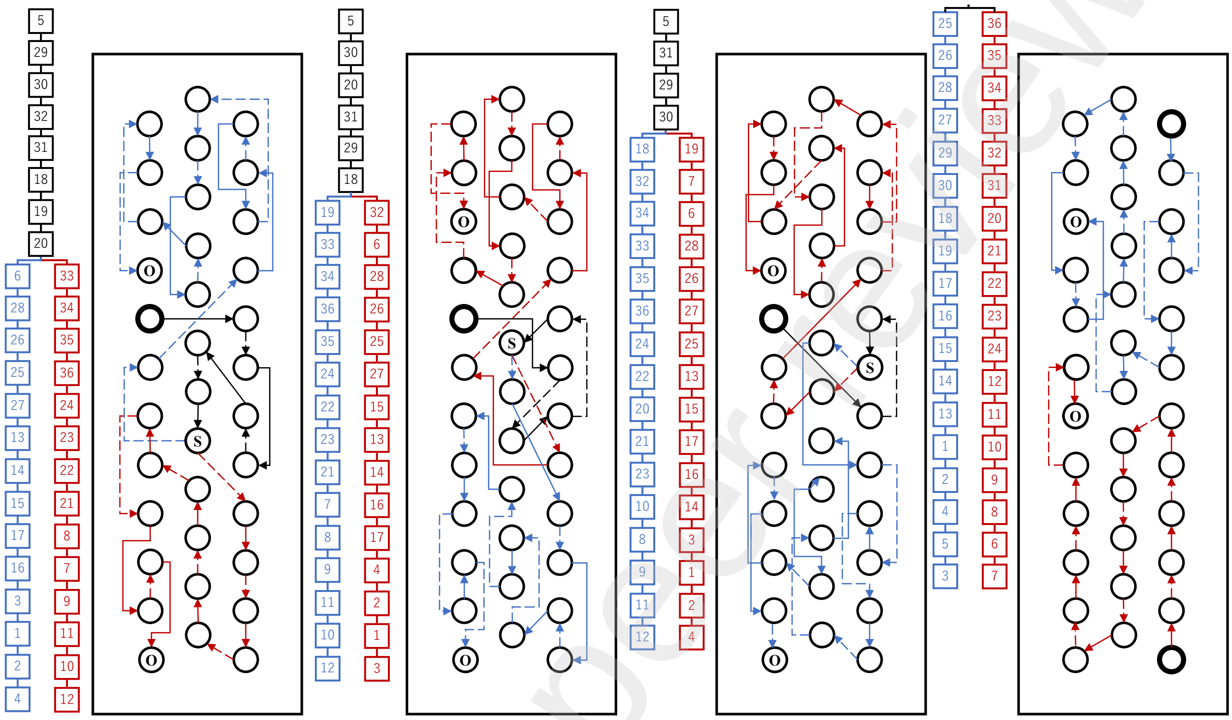

(a) (b) (c) (d)

Fig. 10: Optimized refrigerant circuitries for R454C under different cooling capacity conditions: (a) 4, (b) 6, (c) 8, (d) 10 kW

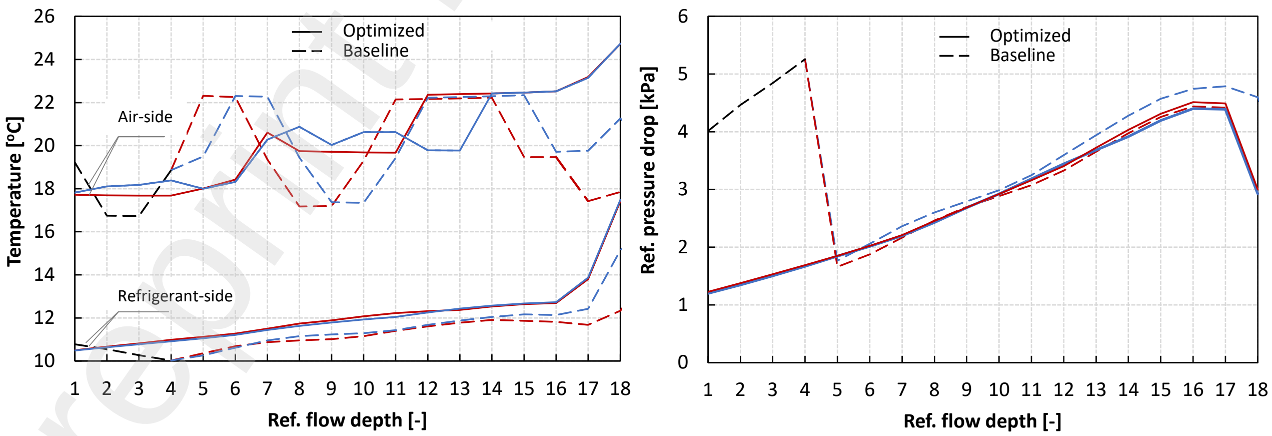

Fig. 11: Local refrigerant pressure drop and refrigerant/air temperatures for R454C for a 10-kW cooling capacity

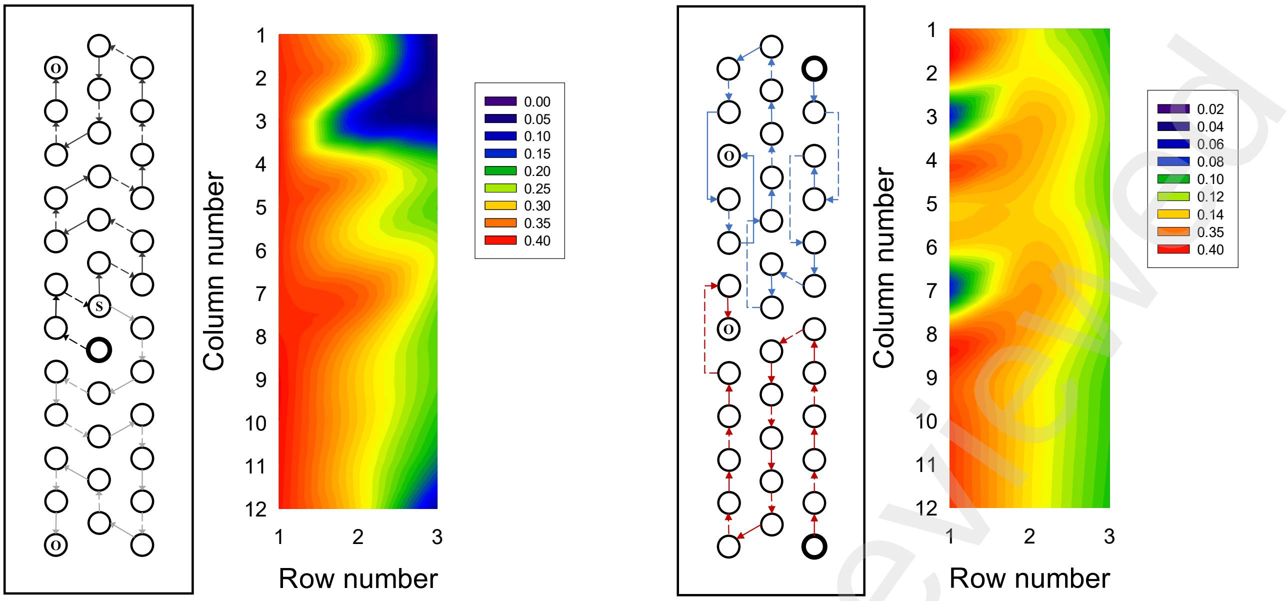

Fig. 12. Contours of the local heat transfer rate Q [kW] for the R454C-refrigerant (a) baseline and (b) optimized circuitries for a 10-kW cooling capacity

The fundamental difference between a pure refrigerant and a zeotropic mixture such as R454 is notably revealed by the results shown in Fig. 13. The circuitry optimization for R32 reduced the thermal entropy generation over the entire investigated cooling capacity range, and the entire entropy generation benefits compensated for the increase in friction entropy generation. It is worth noting that, given the conflicting trend between heat transfer and friction irreversibilities, a different refrigerant tube inner diameter can affect the balance between these effects and yield different optimal circuitry configurations [37]. Conversely, the optimized circuitry for the zeotropic refrigerant (R454C) shows a reduction in both entropy generation mechanisms because the lower friction irreversibility yields the possibility of a smaller mean temperature difference between the air and refrigerant by rearranging the tubes in a counterflow configuration that takes advantage of the characteristic temperature glide.

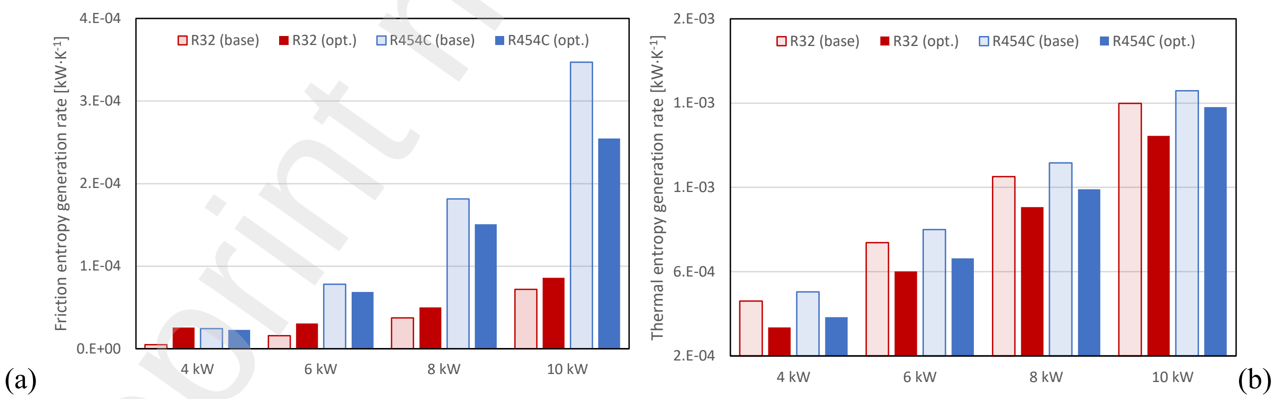

Fig. 13. Comparison between the (a) friction and (b) thermal entropy generation rates for the baseline and optimized circuitries for R32 (red bars) and R454C (blue bars)

Nevertheless, as shown in Fig. 14, the results obtained by minimizing the entropy generation are mirrored by the results obtained by maximizing the COP [22], and a larger entropy generation reduction translates to greater improvements in the COP, especially at a low cooling capacity. The COP improvement and, correspondingly, the entropy generation reduction were larger for R454C. These results demonstrate that the proposed optimization approach can automatize the optimization of the refrigerant path, taking full advantage of the temperature glide characteristic of zeotropic mixtures.

A comparison between the system COP and the optimized evaporator circuitry for two objective functions, namely, maximal COP and minimal entropy generation, is presented in Fig. 15. The close equivalence between the two optimization procedures can be summarized as follows: a 3.86%–8.44%, 3.48%–7.36%, and 4.94%–9.99% COP increase for the R32, R410A, and R454C systems with optimized circuitries, respectively. Among the three refrigerants and evaporator capacities observed, the optimized 4-kW R454C exhibited the largest COP improvement. Additionally, it was found that under these conditions, low-GWP zeotropic mixtures with temperature glide, such as R454C, can achieve a performance comparable to that of R32 and higher than that of R410A following an appropriate refrigerant circuitry optimization.

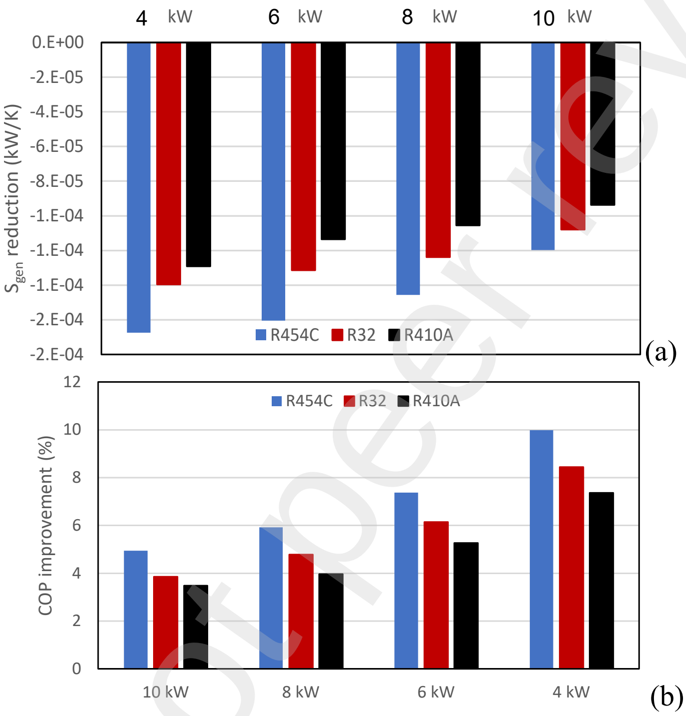

Fig. 14. Representation of the optimization results in terms of the (a) entropy generation rate reduction and (b) relative COP improvement (%) for R32, R410A, and R454C

The proposed thermodynamic refrigerant circuitry optimization for a fine-tube evaporator is an effective methodology for exploiting the beneficial thermodynamic characteristics of the temperature glide of zeotropic refrigerant mixtures. This is achieved by identifying a suitable refrigerant path and determining the appropriate number of circuits to minimize the pressure drop given the target cooling capacity, superheating at the compressor intake, external environment, and indoor space temperatures. This can be interpreted as a thermodynamic cycle optimization under a given heat-source temperature and output capacity, performed by searching for the optimal refrigerant-side topologies of the evaporator to minimize the pressure drop and irreversible losses due to the finite-temperature difference between the air and refrigerant. This procedure automatizes the optimization procedure needed to develop air-conditioning and heat-pump systems that can realize Lorenz-cycle operation in practice.

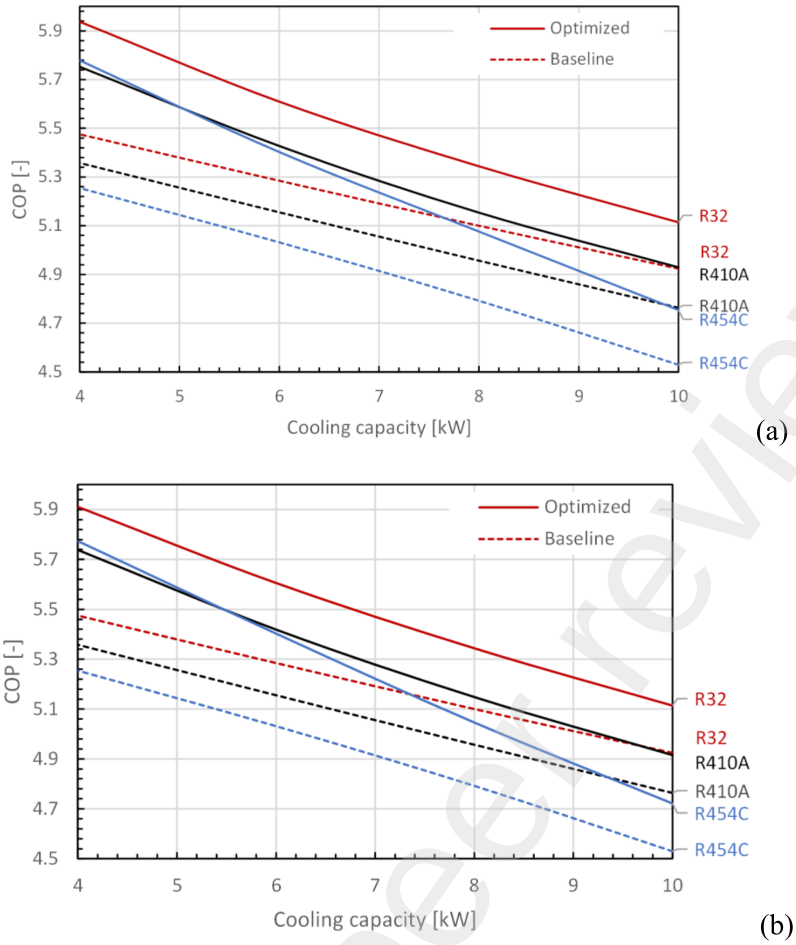

Fig. 15. Optimization results (continuous lines) for (a) maximal COP and (b) minimal entropy generation as objective functions in comparison with the performance of a system adopting the baseline circuitry (dashed lines) for R32, R410A, and R454C.

4. Conclusions

In this study, a new evolutionary method for heat exchanger circuitry optimization that can handle the implementation of genetic operators with unrestrained number and location of splitting and merging nodes was proposed and tested for the thermodynamic optimization of a 36-tube evaporator under representative air-conditioning application conditions. Additionally, an evolutionary search was conducted while adopting algorithms that could exclude unfeasible circuitries and introduce manufacturing constraints.

The performance of different refrigerants, namely, R32, R410A, and R454C, was assessed after minimizing the entropy generation under given heat source and sink boundary conditions, where the calculations converged to a defined superheating degree and output capacity. The optimization results were analyzed, revealing a consistency between the minimum entropy generation and maximum COP. The implementation of the new circuitry optimization algorithm determines efficient heat exchanger topologies by minimizing the friction and finite-temperature-difference heat-transfer irreversibilities. Correspondingly, the pressure drop and mean average temperature difference between the refrigerant and air sides were minimized, thereby reducing the number of ineffective tubes in a superheated state. Consequently, the refrigerant pressure at the evaporator outlet was maximized, the compression ratio was minimized, and the COP was maximized under the given optimization constraints.

The design features for distributing thermodynamic inefficiencies along the refrigerant path were defined for each refrigerant and design condition. For instance, the circuitry optimization for R32 reduces thermal entropy generation over the entire investigated cooling capacity range, and the entire entropy generation benefits compensate for the increase in friction entropy generation. Conversely, the optimized circuitry for the zeotropic refrigerant (R454C) shows a reduction in both entropy generation mechanisms because the lower friction irreversibility yields the possibility of a smaller mean temperature difference between the air and refrigerant by rearranging the tubes in a counterflow configuration, taking advantage of the characteristic temperature glide.

Therefore, this optimization technique is proposed for assessing the performance of next-generation zeotropic refrigerant mixtures. The combination of these methods enables the search for optimal heat exchanger topologies in a way that makes it possible to take advantage of the thermodynamic benefits of non-azeotropic refrigerants by approaching Lorentz-cycle operation. The results demonstrate that non-azeotropic refrigerant mixtures with low GWP may exhibit a higher performance than R410A and a comparable performance to that of R32.

In conclusion, integrating genetic programming and traversing algorithms from graph theory with a numerical simulator yielded an automatized refrigerant-circuitry optimization technique that could benefit the development of high-efficiency products adopting next-generation refrigerants by introducing custom-built features to minimize thermodynamic inefficiencies.

Acknowledgement

This paper is based on results obtained from the project JPNP18005 commissioned by the New Energy and Industrial Technology Development Organization (NEDO).

NOMENCLATURE

	Symbols	n	specific volume ($m^3 \times kg^{-1}$)
COP	Coefficient of performance (-)		Subscripts
h	specific enthalpy ($J \times kg^{-1}$)	a	air
$\dot{m}$	mass flow rate ($kg \times s^{-1}$)	comp	compressor
N	number of tubes	cond	condenser
P	pressure (Pa)	e	evaporator
$\dot{Q}$	heat transfer rate (W)	gen	generation
S	entropy rate ($W \times K^{-1}$)	in	inlet
T	temperature (K)	out	outlet
$\dot{W}$	power (W)	r	refrigerant
	Greek symbols	sat	saturation
h	efficiency (-)	w	tube wall

References

[1] Hou W., Raeisi Fard H., Burns L., Groll E.A., Ziviani D., Braun J.E., 2022. Experimental Investigation of R454C as a Replacement for R410A in a Residential Heat Pump Split System. International Refrigeration and Air Conditioning Conference, West Lafayette, U.S.A., Paper 2482.

[2] Garcia J.C.S., Tanaka H., Giannetti N., Sei Y., Saito K., Houfuku M., Takafuji R., 2022. Multiobjective geometry optimization of microchannel heat exchanger using real-coded genetic algorithm, Applied Thermal Engineering, 202, no. 117821.

[3] Prajapati Y.K., 2019. Influence of fin height on heat transfer and fluid flow characteristics of rectangular microchannel heat sink, International Journal of Heat and Mass Transfer, 137, pp. 1041-1052.

[4] Saleem A., Kim M.H., 2017. Air-side thermal hydraulic performance of microchannel heat exchangers with different fin configurations, Applied Thermal Engineering, 125, pp. 780-789.

[5] Tancabel J., Aute V., Klein E., Lee C.Y., Hwang Y., Ling J., Muehlbauer J., Radermacher R., 2022. Multi-scale and multi-physics analysis, design optimization, and experimental validation of heat exchangers utilizing high performance, non-round tubes, Applied Thermal Engineering, 216, no. 118965.

[6] Wang C.C., Jang J.Y., Lai C.C., Chang Y.J., 1999. Effect of circuit arrangement on the performance of air-cooled condenser. Int. J. Refrigeration 22(4), 275–282.

[7] Liang S.Y., Wong T.N., Nathan G., 2001. Numerical and Experimental Studies of Refrigerant Circuitry of Evaporator Coils, International Journal of Refrigeration, 24(8), pp. 823-833.

[8] Domanski P.A, 1999. Finned-tube evaporator model with a visual interface, presented at the Int. Cong. of Refrig., Sydney, Australia, Sept. 19–24, 1999.

[9] Domanski P.A, EVAP-COND Simulation Models for Finned Tube Heat Exchangers, Gaithersburg, MD, USA: National Institute of Standards and Technology, Building and Fire Research Laboratory, 2003.

[10] Domanski P.A., 1991. Simulation of an evaporator with non-uniform one-dimensional air distribution, presented at the ASHRAE Winter Meet, New York, USA, Jan. 19–23, 1991.

[11] Lee J.H., Bae S.W., Bang K.H., Kim, M.H., 2002. Experimental and numerical research on condenser performance for R-22 and R407-C refrigerants, International Journal of Refrigeration, 25(3), pp. 372–382.

[12] Liang S.Y., Wong T.N., Nathan G.K., 2000. Study on refrigerant circuitry of condenser coils with exergy destruction analysis, Applied Thermal Engineering, 20(6), pp. 559–577.

[13] Ploskas N., Laughman C., Raghunathan A.U., Sahinidis, N.V., 2018. Optimization of Circuitry Arrangements for Heat Exchangers Using Derivative-Free Optimization, Chemical Engineering Research and Design, 131, pp. 16-28.

[14] Jiang H., Aute V., Radermacher R., 2006. CoilDesigner: A general-purpose simulation and design tool for air-to-refrigerant heat exchangers. International Journal of Refrigeration, 29, 601–610.

[15] Li Z., Aute V., Ling J., 2019. Tube-fin heat exchanger circuitry optimization using integer permutation based Genetic Algorithm, International Journal of Refrigeration, 103, pp. 135–144.

[16] Ishaque S., Kim M.H., 2022. Refrigerant circuitry optimization of finned tube heat exchangers using a dual-mode intelligent search algorithm, Applied Thermal Engineering, 212, no.118576.

[17] Domanski P. A., Yashar D., Kim M., 2005. Performance of a Finned-Tube Evaporator Optimized for Different Refrigerants and Its Effects on System Efficiency, International Journal of Refrigeration, 28(6), pp. 820-827.

[18] Li Z., Shen B, Gluesenkamp K.R., 2021. Multi-objective Optimization of Low-GWP Mixture Composition and Heat Exchanger Circuitry Configuration for Improved System Performance and Reduced Refrigerant Flammability, International Journal of Refrigeration, 126, pp. 133-142.

[19] Lee W. J., Kim H.J., Jeong J.H., 2016. Method for determining the optimum number of circuits for a fin-tube condenser in a heat pump, International Journal of Heat and Mass Transfer, 98, pp. 462-471.

[20] Garcia J.C.S., Giannetti N., Varela D.A.B., Varela R.J., Yamaguchi S., Saito K., Berana M.S., 2019. Design of a Numerical Simulator for Finned-Tube Heat Exchangers with Arbitrary Circuitry, Heat Transfer Engineering, 43(19), Selected Papers from the 5th International Symposium on Innovative Materials for Processes in Energy Systems (IMPRES2019), October 20-23, 2019, Kanazawa, Japan.

[21] Giannetti N., Garcia J.C.S., Kim C.H., Sei Y., Enoki K., Saito K., 2023. Circuitry optimization using genetic programming for the advancement of next generation refrigerants, International Journal of Heat and Mass Transfer, 217, no. 124648.

[22] Giannetti N., Garcia J.C.S., Varela R.J., Sei Y., Enoki K., Jeong J., Saito, K., 2021. Development of Assessment Techniques for Next-Generation Refrigerants with Low GWP Values - Fourth report: Efforts and outcomes on heat exchanger optimization in FY 2020, Proceedings of 2021 JSRAE Annual Conference, Tokyo (2021).

[23] Seshimo Y., Fujii M., 1992. Compact Heat Exchangers (in Japanese), Tokyo, Japan: Nikkan Kogyo Shimbun, Ltd., 1992.

[24] Kim N., Youn B., Webb R., 1999. Air-side Heat Transfer and Friction Correlations for Plain Fin-and-Tube Heat Exchangers with Staggered Tube Arrangements, Journal of Heat Transfer, 121(3), pp. 662-667.

[25] Shah M.M., 1982. Chart Correlation for Saturatred Boiling Heat Transfer: Equations and Further Study, AHRAE Transactions, 88(1), pp. 185-196.

[26] Shah M. M., 2015. A method for predicting heat transfer during boiling of mixtures in plain tubes, Applied Thermal Engineering, 89, pp. 812-821.

[27] Dittus F., Boelter L., 1985. Heat Transfer in Automobile Radiators of the Tubular Type, International Communications in Heat and Mass Transfer, 12(1), pp. 3-22.

[28] Muller-Steinhagen H., Heck K., 1986. A Simple Friction Pressure Drop Correlation for Two-Phase Flow in Pipes, Chemical Engineering and Processing: Process Intensification, 20(6), pp. 297-308.

[29] Popiel C., Wojtkowiak J., 2000. Friction Factor in U-Type Undulated Pipe Flow, Journal of Fluids Engineering, 122(2), pp. 260-263.

[30] Domanski P.A., Hermes C., 2006. An Improved Two-Phase Pressure Drop Correlation for 180^o Return Bends, in 3rd Asian Conference on Refrigeration and Air-Conditioning, Gyeongju, Korea, 2006.

[31] Pencheva T., Atanassov K., Shannon A., 2009. Modelling of a roulette wheel selection operator in genetic algorithms using generalized nets, Bioautomation, 13, pp. 257-264.

[32] Bejan A., 1977. The concept of irreversibility in heat exchanger design: counterflow heat exchangers for gas-to-gas applications. J. Heat Transfer, 99, 374-380.

[33] Grazzini G., Gori F., 1988. Entropy parameters for heat exchanger design. Int. J. Heat and Mass Transfer 31, pp. 2547-2554.

[34] Giannetti N., Rocchetti A., Saito K., Yamaguchi S., 2015. Entropy parameters for desiccant wheel design. Appl. Therm. Eng., 75, pp. 826-838.

[35] Giannetti N., Rocchetti A., Lubis A., Saito K., Yamaguchi S., 2016. Entropy parameters for falling film absorber optimization. Appl. Therm. Eng., 93, pp. 750-762.

[36] Kim C.H., Giannetti N., Garcia J.C.S., Sei Y., Enoki K., Saito K., 2023. Circuitry optimization and parametric study on fin-tube evaporators for maximizing COP, Proceedings of 2023 JSRAE Annual Conference, Tokyo.